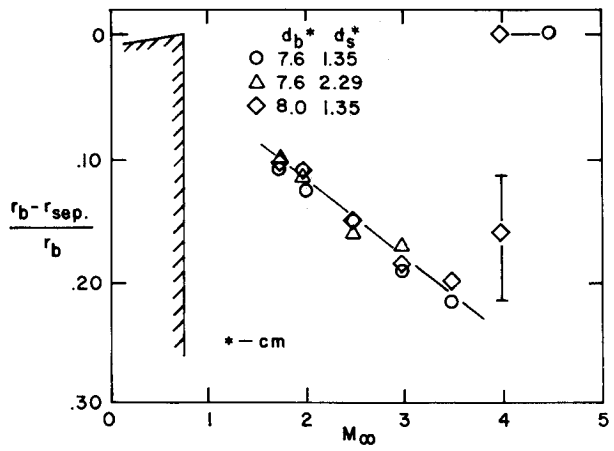

Fig. 5 Mach number effect on location of separation.

Mach number range of 1.75–3.5. Base separation always occurred between the trailing edge corner and the pressure minimum indicating that the radially outward recirculating flow encounters an adverse pressure gradient and then separates. The base pressure gradients near the corner are opposite in sign to those reported by Hama[1]; he interpreted his results as an overexpansion of the flow which turned the corner, encountered an adverse pressure gradient moving away from the corner, and then separated. BRL results at Mach 4.0 and 4.5 showed that base pressure gradients diminished and separation appeared to revert to the corner. For laminar flow, no significant pressure gradients were found to exist (Fig. 3) and oil flow tests indicated separation at the corner. Of the references cited, only the results of Hong and Childs[3] were qualitatively similar to the BRL results. Pitot traverses of Fig. 4 do not show evidence of the shear layer originating from the base; since the oil flow pictures clearly show a base separation, it is concluded that only a slight portion of the boundary-layer flow turns the corner. In contrast, Donaldson's pitot measurements indicate the origin of the separated shear layer is on the base.[2] Attempts at correlating parameters such as Reynolds number and boundary-layer thickness with position of separation were generally not successful; however, the position of separation did appear to be dependent on Mach number as seen in Fig. 5.

Conclusions

1) Separation occurred on the base for turbulent flow and the position of separation is dependent on Mach number. 2) Separation always occurred between the pressure minimum and the trailing edge corner. 3) Separation for laminar flow is at the corner or sufficiently near the corner that the distance cannot be detected by the oil flow method. 4) Theoretical predictions of base separation attribute such phenomena to laminar flows and predict stronger Reynolds number dependence than observed in the present tests.

References

[1] Hama, F. R., "Experimental Studies on the Lip Shock," *AIAA Journal*, Vol. 6, No. 2, Feb. 1966, pp. 212–219.

[2] Donaldson, I. S., "On the Separation of a Supersonic Flow at a Sharp Corner," *AIAA Journal*, Vol. 5, No. 6, June 1967, pp. 1086–1088.

[3] Hong, Y. S. and Childs, M. E., "Experimental Study of Axially-Symmetric Base Flow with Turbulent Initial Boundary Layer at $M_\infty = 2.42$," AIAA Paper 70-796, Los Angeles, Calif., 1970.

[4] Shang, J. S. and Korkegi, R. H., "Investigation of Flow Separation over a Rearward-Facing Step in a Hypersonic Stream," *AIAA Journal*, Vol. 6, No. 5, May 1968, pp. 986–987.

[5] Small, R. D. and Page, R. H., "Turbulent Supersonic Boundary Layer Flow in the Neighborhood of a 90° Corner," *Astronautica Acta*, Vol. 8, Pergamon Press, New York, 1973, pp. 99–117.

[6] Weinbaum, S., "On the Singular Points in the Laminar Two-Dimensional Near Wake Flow Field," *Journal of Fluid Mechanics*, Vol. 33, Pt. I, 1968, pp. 38–63.

[7] Roache, P. J. and Mueller, T. J., "Numerical Solutions of Laminar Separated Flows," *AIAA Journal*, Vol. 8, No. 3, March 1970, pp. 530–538.

[8] Kayser, L. D., "Experimental Study of Separation From the Base of a Cone at Supersonic Speeds," Masters Thesis, May 1974, Univ. of Delaware, Newark, Del.

Effect of Stress on the Directions of Stiffness Extrema

A. A. G. Cooper*
Babcock & Wilcox Company, Alliance, Ohio

Nomenclature

S_{ij}* = component of compliance tensor referred to x, y axes
U = $2x$ elastic energy stored in unit element
V_2, V_3 = see Appendix
p = $V_3(1-s)/[V_2(1+s)]$
s = σ_b/σ_a, $-1 \leqq s \leqq 1$
x, y = principal stress directions
θ = orientation of 1(2) axis with respect to $x(y)$ axis
σ_a, σ_b = principal stresses, $|\sigma_a| \geqq |\sigma_b|$
1, 2 = axes of material symmetry

Introduction

In some orthotropic materials the directions of maximum and minimum stiffness for a given state of stress depend not only on the elastic constants of the material but also on the applied stresses.[1,2]

This Note is a summary of an analysis of this behavior. The analysis is based on the use of stored elastic energy as a measure of stiffness. It is similar to but more detailed than the analysis given in Ref. 2 which resulted from the derivation of an optimality condition for reinforcement patterns in fiber reinforced composite structural components.

Analysis

Let a two-dimensional orthotropic unit element be subjected to a state of stress which is represented by its principal stresses σ_a and σ_b acting in the principal stress directions x and y, respectively. Let the 1 and 2 axes be the major and minor axis, respectively, of material symmetry. The orientation of the 1(2) axis with respect to the $x(y)$ axis is θ. The elastic properties are assumed to be the same in tension and compression.

The elastic stress energy stored in the unit element is adopted as a measure of the stiffness. With the stresses given, maximum (minimum) stiffness corresponds with minimum (maximum) elastic stress energy. (For a given uniaxial state of stress, stiffness and elastic stress energy are inversely proportional.)

The elastic stress energy stored in the unit element is given by

$$U/2 = \sigma_a{}^2[S_{11}{}^* + 2sS_{12}{}^* + s^2S_{22}{}^*]/2 \qquad (1)$$

To find the orientations for which the elastic energy attains an extremum, the first derivative of U with respect to θ is set equal to zero. The nature of the extremum is then determined from the sign of the second, third, and fourth derivatives at those values of θ for which the first derivative is zero.

From Eq. (1) and the transformation of S_{ij}* (see Appendix), the condition that the first derivative U' be zero gives

$$U' = -8\sigma_a{}^2 \sin(2\theta)[V_2(1-s^2) + V_3(1-s)^2 \cos(2\theta)] = 0 \qquad (2)$$

Received May 10, 1974; revision received June 24, 1974.
Index categories: Structural Composite Materials (Including Coatings); Structural Static Analysis.

* Project Engineer, Advanced Composites Department. Member AIAA.

and hence

$$\sin(2\theta) = 0 \tag{3}$$

and, if

$$s \neq \pm 1,\ \cos(2\theta_i) = -1/p \tag{4}$$

From Eq. (3) it follows $\theta = 0, \pm\pi/2, \pi$ which is the trivial case of the 1, 2 axes coinciding with the x, y or y, x axes. For $s \neq \pm 1$ the nontrivial case of an intermediate orientation $(\pm\theta_i \pm \pi)$ is given by Eq. (4). An intermediate orientation is possible if in Eq. (4) $p \geqq 1$ or $p \leqq -1$, but if $p = \pm 1$ Eq. (4) is equivalent to Eq. (3) and therefore an intermediate orientation requires $p > 1$ or $p < -1$.

The second, third, and fourth derivatives of U with respect to θ are readily found from Eq. (2) and given by Eqs. (5–7)

$$U'' = -16\sigma_a^2 V_2(1+s)[p\cos(4\theta) + \cos(2\theta)] \tag{5}$$

$$U''' = 32\sigma_a^2 V_2(1+s)[2p\sin(4\theta) + \sin(2\theta)] \tag{6}$$

$$U'''' = 64\sigma_a^2 V_2(1+s)[4p\cos(4\theta) + \cos(2\theta)] \tag{7}$$

From Eqs. (2, 3, 5–7) it follows

$$\text{if}\quad p \geqq -1,\ U(\theta = 0, \pi)\quad \text{is minimum} \tag{8}$$

$$\text{if}\quad p \leqq 1,\ U(\theta = \pm\pi/2)\quad \text{is maximum} \tag{9}$$

That is: $-1 \leqq p \leqq 1$ relates to the trivial case of the 1, 2 axes coinciding with the x, y or y, x axes.

From Eqs. (2, 4, and 5) it follows that

$$\text{if}\quad p > 1,\ U(\theta = \pm\theta_i \pm \pi)\quad \text{is maximum} \tag{10}$$

$$\text{if}\quad p < -1,\ U(\theta = \pm\theta_i \pm \pi)\quad \text{is minimum} \tag{11}$$

From Eq. (1) and the transformations given in the Appendix it can be found that

$$U(\pm\theta_i \pm \pi) - U(0, \pi) = -2\sigma_a^2 V_2(1+s)(p+1)^2/p$$

and

$$U(\pm\theta_i \pm \pi) - U(\pm\pi/2) = -2\sigma_a^2 V_2(1+s)(p-1)^2/p$$

With these expressions or with Eqs. (5, 6, and 7) it can be shown that the extrema given by Eqs. (10) and (11) are absolute.

For $s = 0$ (uniaxial tension or compression), θ_i is independent of the stress and Eq. (4) reduces to

$$\cos(2\theta_i) = -V_2/V_3 \tag{12}$$

Writing Eq. (12) in terms of engineering constants (see Appendix) and substituting into Eqs. (8–11) give the conditions for orientations of modulus extrema of orthotropic materials derived in Refs. 3 and 4.

For $s = 1$, U is independent of θ. This case represents a hydrostatic state of stress. In the hydrostatic state of stress there is an infinite number of principal stress directions and therefore θ has no meaning. Likewise, if the material is isotropic ($V_2 = 0$, $V_3 = 0$) there is an infinite number of axes of material symmetry and θ is meaningless.

If $s = -1$ (pure shear at $\pm 45°$), Eq. (2) reduces to

$$U' = -16\sigma_a^2 V_3 \sin(4\theta) \tag{13}$$

and the second derivative is

$$U'' = -64\sigma_a^2 V_3 \cos(4\theta) \tag{14}$$

From Eqs. (13) and (14) it follows that for $s = -1$, U is maximum and therefore the stiffness is minimum at $\theta = 0, \pm\pi/2, \pi$ if $V_3 > 0$ or at $\theta = (\pm\pi/4 \pm \pi)$ if $V_3 < 0$. And U is minimum and therefore the stiffness is maximum at $\theta = 0, \pm\pi/2, \pi$ if $V_3 < 0$ or at $\theta = (\pm\pi/4 \pm \pi)$ if $V_3 > 0$.

Figure 1 shows θ_i as a function of s for unidirectional Boron/Epoxy (B/Ep), curve A, and for the B/Ep laminate mentioned by Chu,[4] curve B. In Chu's laminate, 40% of the fibers is in the 1-direction and 60% is at $\pm 45°$ with respect to the 1-direction; the layup is here assumed to be balanced. The properties of the B/Ep were taken from Ref. 5 Table 1.2.1-1, and those of Chu's laminate from Ref. 5, Figures 1.2.2-6, -8, and -9.

For the θ_i interval shown in Fig. 1 for unidirectional B/Ep the stiffness is minimum, since $p > 1$. For maximum stiffness $\theta = 0, \pi$; the directions of the (absolute) stiffness minimum and the stiffness maximum are not orthogonal in this interval. In the

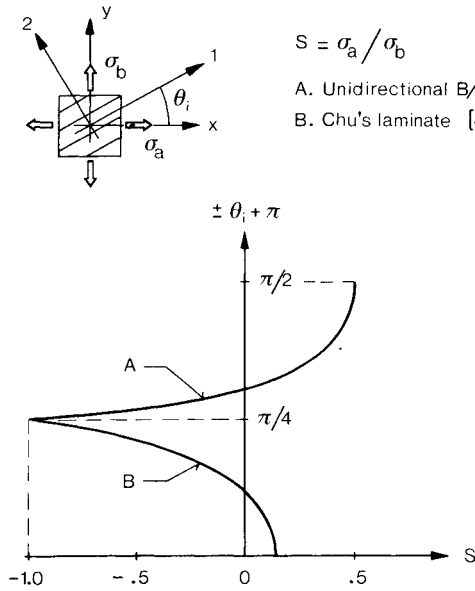

Fig. 1 θ_i as function of s for minimum (A) and maximum (B) stiffness.

θ_i interval shown for Chu's laminate, the stiffness is maximum since $p < -1$. For minimum stiffness $\theta = \pm\pi/2$; the directions of the (absolute) stiffness maximum and the stiffness minimum are not orthogonal in this interval.

If θ_i is the orientation of the principal stress directions (with respect to the axes of material symmetry) the shear strain associated with the principal stresses is zero; thus the principal strain directions coincide with the principal stress directions.

An analysis of the effect of strain on the stiffness directions can be made similar to the present analysis, using the strain energy rather than the stress energy as a measure of the stiffness.

Conclusion

In some orthotropic materials the directions of maximum and minimum stiffness for a given state of stress depend on the elastic constants of the material and also on the applied stresses. The orientation of the axes of material symmetry with respect to the principal stress directions can be expressed in terms of the elastic constants and the ratio of the principal stresses. From this expression, conditions have been derived for maximum and minimum stiffness directions. One of the two directions always coincides with one of the axes of material symmetry. The directions of minimum and maximum stiffness, which are principal stress directions, are also principal strain directions.

Appendix

The following transformations of S_{11}^*, S_{12}^*, and S_{22}^* were taken from Ref. 6 with some changes in notation.

$$S_{11}^* = V_1 + 4V_2\cos(2\theta) + V_3\cos(4\theta)$$

$$S_{22}^* = V_1 - 4V_2\cos(2\theta) + V_3\cos(4\theta)$$

$$S_{12}^* = V_4 - V_3\cos(4\theta)$$

$$V_1 = (3S_{11} + 3S_{22} + 2S_{12} + S_{66})/8 = (3/E_1 + 3/E_2 - 2\nu_{12}/E_1 + 1/G_{12})/8$$

$$V_2 = (S_{11} - S_{22})/8 = (1/E_1 - 1/E_2)/8$$

$$V_3 = (S_{11} + S_{22} - 2S_{12} - S_{66})/8 = (1/E_1 + 1/E_2 + 2\nu_{12}/E_1 - 1/G_{12})/8$$

$$V_4 = (S_{11} + S_{22} + 6S_{12} - S_{66})/8 = (1/E_1 + 1/E_2 - 6\nu_{12}/E_1 - 1/G_{12})/8$$

E_1, E_2, ν_{12}, and G_{12}, respectively, are the elastic moduli, Poisson's ratio and the shear modulus, respectively, referred to the axes of material symmetry which are assigned such that $E_1 > E_2$.

References

[1] Cooper, A. A. G. and Wu, E. M., "Trajectorial Fiber Reinforcement of Composites," *Proceedings of the Sixth St. Louis Symposium on Composite Materials*, Washington Univ.-Monsanto Co. Association, St. Louis, Mo., 1972, pp. 377–382.

[2] Cooper, A. A. G., "Trajectorial Fiber Reinforcement of Composite Structures," D.Sc. thesis, 1972, Washington Univ., St. Louis, Mo.

[3] Fokin, A. G. and Shermergor, T. D., "Effect of Orientation of Reinforcing Fibers on the Elasticity Moduli of Materials," *Mechanics of Solids*, Vol. 2, No. 2, 1971, pp. 63 66; Also see *Inzhenernyi Zhurnal Mekhanika Tverdogo Tela*, Vol. 2, No. 2, 1967, pp. 93–98.

[4] Chu, K. S., "Some Characteristics of Laminated Filamentary Composites," *AIAA Journal*, Vol. 9, No. 7, July 1971, pp. 1407–1408.

[5] *Advanced Composites Design Guide*, 3rd ed., Air Force Materials Lab., Wright-Patterson Air Force Base, Ohio, Nov. 1971.

[6] Wu, E. M., "Composite Materials," Course ME654, Fall 1968, Washington Univ., St. Louis, Mo.

Hypergolic Ignition of Rocket Propellants with Nitric Acid Containing Dissolved Nitrogen Tetroxide

U. C. DURGAPAL* AND V. K. VENUGOPAL†

Birla Institute of Technology, Ranchi, India

Introduction

LOW ignition delay in hypergolic bipropellants is a great advantage in the design of liquid rocket engines as it helps to eliminate undesirable pressure peaks. Red fuming nitric acid (RFNA) is hypergolic with a number of fuels and many investigations have been carried out to determine the manner in which the ignition delay is influenced by added catalysts, water content of the acid, temperature of the propellants, etc.[1-4] However, no data has been reported on the effect of concentration of dissolved nitrogen tetroxide (N_2O_4) on the ignition delay. The present investigation was carried out mainly for that purpose. Results presented herein show that increase in the concentration of dissolved N_2O_4 in nitric acid invariably results in a decrease in ignition delay. The magnitude of the effect depends on the chemical nature of the fuel which determines the mechanism of preignition reactions.

Materials

The fuels selected for study were an aromatic amine xylidine (mixed isomers), an aliphatic amine triethylamine (TEA) and a hydrazine derivative, unsymmetrical dimethyl hydrazine (UDMH). Chemically pure samples of these fuels were used. Commercial nitric acid containing 1.97% by weight of dissolved N_2O_4 was used as such as oxidizer. N_2O_4-free oxidizer was prepared by heating the commercial acid in an open dish at 60°C for half an hour. Oxidizer containing higher percentage of N_2O_4 was prepared by bubbling dry N_2O_4 through chilled commercial acid, the dry N_2O_4 being obtained by heating concentrated nitric acid with copper turnings in a flask and passing the gas produced in the reaction over phosphorous pentoxide. Different concentrations of dissolved N_2O_4 were obtained by passing the gas for different lengths of time through the chilled acid. The concentration of N_2O_4 in the acid samples was determined by a method described by Welcher.[5]

Ignition Delay Measurements

A simplified form of the modified open cup tester described by Ladanyi and Miller[6] was used for these experiments. All testing was done at room temperature (21°±2°C) and therefore the cooling arrangement was not provided. The fuel was loaded in the test tube and the oxidizer was kept in the ampule; the advantage being that once the ampule was flame sealed there was no possibility of escape of N_2O_4 and consequent change in composition of the oxidizer. To ensure uniformity, as soon as a particular sample of acid was prepared, a large number of ampules were filled up and sealed. Some of these were used for chemical analysis to determine the concentration of dissolved N_2O_4 and the rest were used for ignition delay experiments. Ignition delay was measured using a photocell and oscilloscope arrangement. The starting signal was obtained at the instant of contact by impact of the drop weight on the head of crush rod. The fore end of the drop weight carried a metal pin which made contact in a mercury well provided on the head of the crush rod to ensure stable electrical contact. It was found that in the absence of such an arrangement the oscilloscope trace was unsteady and difficult to read due to vibrations accompanying the impact.

Results and Discussion

The experimental results are given in Table 1. In case of xylidine a slow uniform decrease in ignition delay is observed with an increase in concentration of N_2O_4 in the oxidizer. It was also observed that ignition was preceded by the evolution of a lot of smoke. A large carbonaceous residue was left which decreased with increase in concentration of N_2O_4. In case of TEA, the presence of a small amount of N_2O_4 in nitric acid brings down the ignition delay enormously and a further increase in concentration of N_2O_4 does not have any effect. In the case of UDMH, though the ignition delay was reduced but the effect was not at all significant. The ignition in the case of UDMH was accompanied by a loud report, like the sound of a small explosion, the intensity of this sound increasing noticeably with an increase in concentration of N_2O_4. This may be similar to the popping phenomena[7] observed in case of N_2O_4-Hydrazine system due to extreme reactivity of the propellants and may be significant from the point of view of injector design in practical systems using UDMH-RFNA combination.

The cause for the different effects on the ignition delay in the three cases most probably lies in the difference in the manner in which N_2O_4 influences the mechanism of the preignition processes. It would therefore be interesting to analyse the relative importance of nitric acid and N_2O_4 in these processes.

Table 1 Ignition delay data

Concentration of N_2O_4 dissolved in nitric acid, wt %	Average Ignition Delay[a] Xylidine[b] $F/O = 1.5$ sec	TEA $F/O = 4$ m sec	UDMH $F/O = 0.25$ m sec
0	2.1	68.66	4.83
1.97	2.0	24.66	4.76
8.35	1.5	23.66	4.70
15.23	1.33	23.52	4.40
21.30	1.17	23.33	4.20

[a] In all cases 1 ml of oxidizer was taken in the ampule. The fuel to oxidizer ratios (F/O) used are those which gave minimum ignition delay in diagnostic measurements with acid containing 1.97% N_2O_4.

[b] In case of Xylidine a stop watch was used for measurement, because of long time intervals involved and because of the fact that a large amount of smoke was evolved prior to ignition, fouling the inner wall of the test tube and rendering the signal to photocell very weak.

Received May 13, 1974. This work formed part of the M.Sc. (Eng.) Thesis submitted by V. K. Venugopal to Ranchi University in 1973. Thanks are due to the Government of India, Ministry of Defence, for the award of a fellowship for the duration of the work.

Index categories: Fuels and Propellants, Properties of; Liquid Rocket Engines.

* Visiting Professor, Department of Space Engineering and Rocketry.

† Research Fellow, Department of Space Engineering and Rocketry; presently Senior Scientific Officer, Defence Research and Development Laboratory, Hyderabad, India.